PROCEEDINGS OF THE 14TH SYMPOSIUM ON THE GEOLOGY OF THE BAHAMAS AND OTHER CARBONATE REGIONS

Edited by
Fredrick D. Siewers and Jonathan B. Martin

Production Editor:
Fredrick D. Siewers

Gerace Research Centre
San Salvador Island, Bahamas
2010

Front Cover Photograph – "Kelly and the Veggiemorphs" courtesy of Jon Martin

Back Cover Photograph – "Luigi" courtesy of Erin Rothfus

A & A Printing Inc., Tampa, FL

ISBN 0-935909-90-7

PETROGRAPHIC, GEOCHEMICAL AND MAGNETIC PROPERTIES OF CARBONATE ROCK FORMATION AND LOW TEMPERATURE DIAGENETIC ALTERATION OF UNCONSOLIDATED SEDIMENTS ACCOMPANYING THE FORMATION OF GAS HYDRATE DEPOSITS

Tark Hamilton
Camosun College
3100 Foul Bay Rd. Victoria
BC V8P 5J2, Canada

Lionel Esteban
Now at: CSIRO, Petroleum Resources ARRC
26 DickPerry Ave.
Kensington, WA Perth 6151

Randolph J. Enkin
Geological Survey of Canada-Pacific
9860 West Saanich Road
Sidney, BC, Canada, V8L 4B2

ABSTRACT

Unconsolidated sediments were examined in cores from three gas hydrate (GH) settings: permafrost in fluvial-deltaic silts and sands in the Western Canadian Arctic (Japex et al. Mallik 5L-38 in 2002); diamictons and hemipelagics in the Cascadia accretionary wedge west of Vancouver Island (IODP Exp.311 in 2006); and marine sands and hemipelagics from the Bay of Bengal (NGHP Exp.01 in 2007). In all three settings, adjacent to the GH-bearing layers are diagenetically cemented bands are found which contain carbonate crusts, limestone layers, veins with authigenic carbonate and massive sulfide. These cements have distinctive textures, infilling available inter- and intra-granular porosity, forming multiple cross cutting veins and overprinting and disrupting primary sedimentary textures with isolated idiomorphic crystals (rhombs, blades, cubes, framboids). The diagenetic minerals grew so extensively in inter-granular pore space that the original sediments have become inflated, rafting apart and even fracturing and infilling original detrital grains. Carbonates are often nucleated in the center of pores and grew concentrically towards the grains, rather than nucleating on grain contacts. In some samples, cement minerals occur in curvi-planar masses suggesting growth on bacterial films in fluid-filled fractures. Sediments are sometimes blackened with the deposition of reduced carbon spherules. Cements also exhibit bacterial growth texture in-filling microporosity inside foraminifera and woody plant fragments. The observed diagenesis is explained by physical-chemical processes involving brine concentration by solute exclusion, and bacterial processes involving anaerobic metabolism of methane producing carbonate and sulfide ions. The freezing which accompanied GH crystallization quickly removed pure water, froze the sediments into an impermeable solid and expelled more concentrated brines into the adjacent less permeable strata to the point of inducing fracture formation. Adjacent to the GH plug or cap, the remaining pore fluids became saline, strongly reducing and charged

with methane. Given the abundance of methane at this point, bacterial oxidation of methane ensued adjacent to the GH layers producing bicarbonate and sulfide ions by sulfate reduction. Reduction of iron in pore fluids led to precipitation of iron sulfides, recording an observable diagenetic magnetic signal. Sediments in deep, low temperature environments with significant methane flux and GH formation undergo an early kind of diagenesis and cementation that forms well before lithification of the more porous and permeable facies (like sand/silt) nearby or in adjacent parts of the stratigraphic column. The introduction of carbonates, sulfides and reduced carbon has significant implications for the environments of formation and interpretation of early diagenetic carbonate cements, sedimentary massive sulfide deposits and fine grained euxinic shales.

INTRODUCTION

Ice-like deposits of gas hydrate (GH) constitute the largest hydrocarbon reservoir on Earth (Kvenvolden, 1993). They represent an enormous source of methane as a potential fossil fuel (Lee and Holder, 2001), and possibly the most significant source or sink for greenhouse gases (Paull et al., 1991; Haq, 1998). Gas hydrates form in environments which are associated with physical, chemical and biological conditions conducive to the formation of diagenetic mineral cements. Recent papers discussed diagenetic mechanisms in sediments which host low temperature cements and authigenic mineralization induced by GH formation (Enkin et al., 2007; Esteban et al., 2010). This type of early diagenetic cementation causes increased rigidity and reduced permeability of sediments adjacent to GH deposits.

The conditions to form gas hydrates include a methane source (thermogenic or biogenic) in suitably high concentration to form GH. As methane accumulates, it also provides a substrate or food source for anaerobic, methanotropic archaebacteria to oxidize methane and a suit-

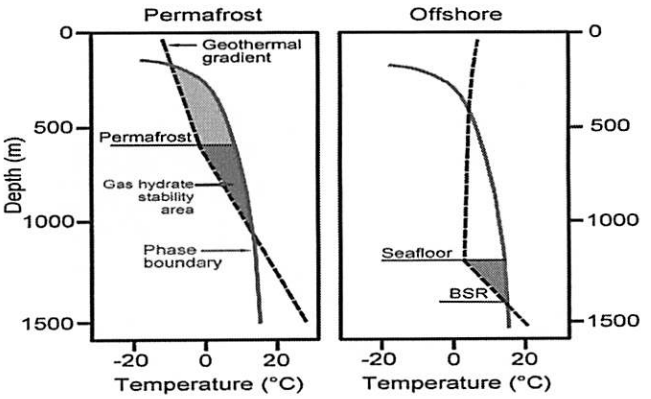

Figure 1: Gas hydrate (GH) stability zone beneath continental permafrost and in offshore regions related to pressure (i.e. depth) and temperature within the sediments. The empirical GH stability zone, shaded dark, requires low enough temperature and high enough pressure to trap small energetic methane molecules within the lattice of the water-ice structure which forms the cage of the clathrate. GH can nucleate anywhere between the geotherm and the phase boundary for methane trapped in ice. In the periglacial continental setting with a depressed geotherm, there is also a permafrost ice field occupied by excess water ice at too low of a pressure to form GH. Above the phase boundary the temperature is too high and the pressure is too low to trap methane in GH and it occurs as free gas. In marine settings methane concentration is generally too low as a dissolved gas for GH to form within the water column. In areas of concentrated methane venting, GH can form in the lower water column, but its low density causes it to rise, like upwards directed snow, and dissociate as it decompresses and warms up. Only where it is trapped in denser, cohesive sediment can it accumulate. The BSR represents the bottom simulating reflector and corresponds to the base of the gas hydrate stability zone as detected seismically.

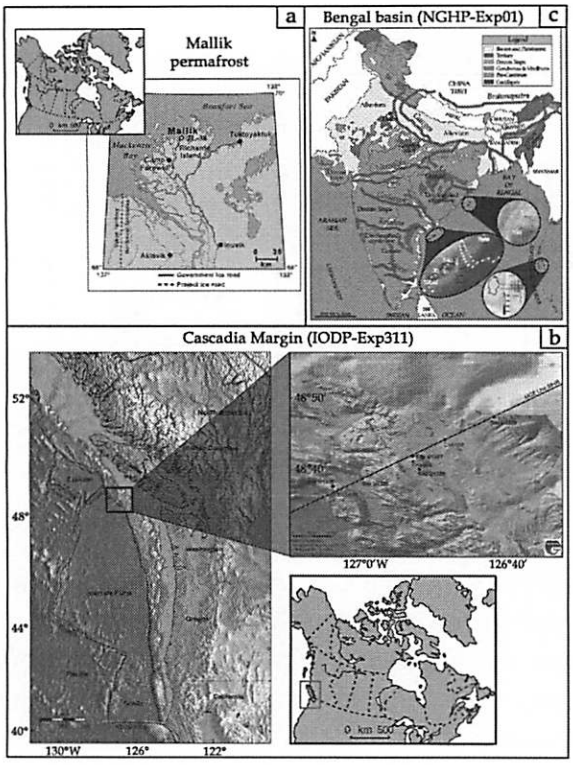

Figure 2: Locations of the three gas hydrate investigations: (a) in permafrost, Northwest Territories (Canada, Mallik, sites 2L-38 and 5L-38), and offshore in: (b) the active Cascadia margin convergent (west of Vancouver Island, Canada, IODP exp311, 5 sites) and in (c) the passive margin of the Bengal basin (India, NGHP-exp01, 8 sites).

Table 1: Geological setting aspects from three sites hosting gas hydrates: Mallik (permafrost), Cascadia Margin (active margin) and Bengal Fan (passive margin).

Property/Locality	Mallik	Cascadia	Bengal Fan
Tectonic setting	Foreland basin	Active margin	Passive margin
Geological setting	Mackenzie Delta	Accretionary Wedge	Deep sea fan
Substrate	Fluvial-Deltaic Quartz sand & silt Coals	Glacial diamicton Turbidites Hemipelagic ooze	Lithic sands & silts Turbidites Hemipelagic ooze
Gas hydrate type	Permafrost	Submarine	Submarine
Methane Source	Thermogenic	Thermogenic Biogenic	Thermogenic Biogenic
Carbonate Cements	Mn-Calcite Dolomite Siderite	Calcite	Calcite
Sulphide Cements	Mn-Pyrite Smythite	Pyrite (at seabed) Greigite	Pyrite Greigite/Smythite
Amorphous Carbon	Present in veins	Present near seafloor	Present in sands
Cement Textures	Veins Disseminated Inflationary	Veins, crusts, mounds Disseminated Pore infilling	Disseminated Pore infilling
Water Source	Solute exclusion Basement, advective	Solute exclusion Wedge & seawater	Solute exclusion Compaction
Lithification	Some layers	Crusts & veins	Veins & patches

able environments for other associated halophile species which reduce electron receptors such as sulfate or ferric ions. This must occur in the GH stability field (Fig. 1) at suitably low temperature and high pressures to form the clathrates (Sloan, 1998). Extensive diagenetic processes occur in the presence of oxidized chemical species in the pore water such as sulfur (S^{6+}) in sulfate ions (SO_4^{2-}), ferric ions (Fe^{3+}), manganese ions (Mn^{3+}, Mn^{4+}) or brines containing other oxidized elements especially the d- and f- block metals. The brines can become saturated enough by solute exclusion during GH freezing to precipitate specific mineral phases including the carbonates, (calcite, dolomite, siderite) and sulfides, (greigite, pyrite).

In order to understand some of the significant processes involving GH deposits and diagenetic carbonate formation, locations have been chosen from three different geological settings (Fig. 2; Table 1): Mallik (Mackenzie delta, Northwest Territories of Canada) in a permafrost affected foreland basin, Cascadia Margin (west coast of Vancouver Island in Canada) on an active accretionary wedge, and the Krishna-Godavari basin (KGB of the Bengal fan) on India's passive margin. The geological settings are compared with geochemical and petrographic analysis to emphasize the main parameters which drive the formation of carbonates in the GH regime. At all three locations, sediments were regularly sampled along the boreholes for laboratory magnetic measurements and for petrographic analysis of thin sections. Selected intervals, representing different lithologies, facies, and diagenetic cements were also submitted for multi-element geochemical studies on leachates.

GEOCHEMICAL PARAMETERS OF SULFIDE AND CARBONATE CEMENT PROCESSES IN MARINE SEDIMENTS

Slight variations in fluid chemistry and/or flux will interact with in-situ ions from bacterial reduction to precipitate ''early diagenetic" cements, including carbonates, reduced carbon and/or magnetic sulfide minerals. The cements can be tracked by their physical properties (e.g., magnetism and electrical resistivity). In marine sediments, sea-water sulfate ions diffuse down from the sea floor and become reduced across the same depth range in which methane fluxing from below becomes oxidized. The depth of this sulfate-methane transition zone (SMTZ) is controlled not only by sulfate concentrated in the pore water at deposition or by diffusion (if it is very near the seabed) but also by sulfate flux from deeper sources including advected fluids and solutes expelled to the margins of GH deposits or in fractures which lead to or emanate from them. The SMTZ usually occurs on the order of 10 to 30 meters below the seabed, but may be shallower where methane flux is rapid and/or the diffusion of seawater sulfate is slow and/or the sedimentation rate is slow (Hensen et al., 2003; Riedinger et al., 2005). The methane concentration and its flux are also a determinant factor in the SMTZ depth as more methane leads to greater anaerobic sulfate reduction. The sulfate and methane flux and their concentrations are controlled by the permeability of the sediment pile and fracture systems which cut it. Two important chemical reactions occur in marine sediments under GH regime:

1) Anaerobic methane oxidation (Blair and Aller, 1995; Fu et al., 2008) leads to the reduction of sulfate to sulfide or bi-sulfide ions along with the formation of carbonate or bicarbonate ions such as:

(eq.1) $CH_4 + (SO_4)^{2-}_{(aq)} \Longrightarrow (HS)^-_{(aq)} + (HCO_3)^-_{(aq)} + H_2O$

(eq. 2) $Ca^{2+}_{(aq)} + (CO_3)^{2-}_{(aq)} \Longrightarrow CaCO_{3(s)}$

Equation 1 is accomplished by an assemblage of anaerobic methanotropic archea-bacteria and sulfate reducing bacteria (or iron reducing bacteria) which live off of the partially oxidized

organic products of the former group. Equation 2 is a familiar precipitation reaction of carbonates dependant on concentrations. As with sulfate, Fe and Mn oxides can also be important electron acceptors, especially near to oxidized seabeds or from detrital oxide minerals as discussed below. GH-bearing sediments are frequently observed to contain multiple sulfur species including: hydrogen sulfide gas, bi-sulfide ions, native sulfur-polymers and various iron sulfide minerals. This situation is uncharacteristic of either a simple inorganic reaction or a system at equilibrium. For this reason, descriptive chemical equations are more of a global statement than an indication of a specific reaction or an individual process.

Pore fluid carbonate or bicarbonate is concentrated via solute exclusion as GH formation takes up pure water. With suddenly concentrated Ca^{2+}, Mg^{2+}, Fe^{2+}, Mn^{2+} ions from solute exclusion or brine flux, carbonate cements can precipitate adjacent to GH deposits, forming veins or other pore infillings. Where methane vents to the seabed and oxygen or oxidized species and calcium ions are abundant, cold carbonate mounds can form from a variety of inorganic or microbial processes as well as from carbonate-shelled invertebrates associated with an assemblage of symbiotic methanotropic bacteria. As the setting for these mounds off of Vancouver Island is cold, deep (>1300 m) and undersaturated for both calcite and aragonite (Chen et al., 1988), it is very atypical geological environment compared to most carbonates.

2) Partially reduced iron in pore waters combine with sulfide to form greigite via a precipitation reaction such as:

(eq.3) $(Fe^{2+})_{(aq)} + 2(Fe^{3+})_{(aq)} + 4(S^{2-})_{(aq)} \Longrightarrow Fe^{2+}Fe^{3+}{}_2S_{4\,(s)}$

Other investigators prefer to describe the formation of magnetic iron sulfide minerals via a precursory (Krupp, 1994) magnetic iron deficient mono-sulfide mineral such as mackinawite (equation 4: Berner, 1970; Pyzic and Somer, 1981) and subsequent sulfidation reactions to ferrimagnetic greigite and eventually to paramagnetic pyrite (equations 5 and 6: Sweeney and Kaplan, 1973).

(eq.4) $(Fe^{2+})_{(aq)} + (HS)^-_{(aq)} \Longrightarrow FeS_{(s)} + H^+_{(aq)}$ (mackinawite, fine grained iron monosulfide)

(eq.5) $3FeS_{(s)} + S^0_{(aq)} \Longrightarrow Fe^{2+}Fe^{3+}{}_2S_{4\,(s)}$ (greigite)

(eq.6) $Fe^{2+}Fe^{3+}{}_2S_{4\,(s)} + 2S^0_{(aq)} \Longrightarrow 3Fe^{2+}S_{2\,(s)}$ (pyrite)

The commonly observed magnetic iron sulfides contain both ferric and ferrous iron whose sum is less than the total potential cation sites in the mono-sulfide structure, like greigite $Fe^{2+}Fe^{3+}{}_2S_4$ (i.e. Fe_3S_4). This mineral has an inverse thiospinel structure which displays similar magnetic properties to oxide-based inverse spinel-type minerals such as magnetite (Fe_3O_4) (Dekkers and Schoonen, 1996). Nonetheless, due to the larger size of the sulfide ion, greigite may be detected and distinguished magnetically from detrital magnetite (Roberts, 1995).

Equation (4) is problematic in that mackinawite is rarely observed and then usually occurs as a surface alteration product on other precursory sulfides. That the sequence of equations represents ordinary iron sulfide paragenesis is also complicated in that iron must be reduced for (4), partially oxidized in (5) then reduced again in (6), all with monotonic increase in sulfidation. This sequence seems unlikely to arise in uniform chemical gradients without the intervention of biological redox processes. Despite this, the redox zone between Fe^{3+}/Fe^{2+} and the SMTZ is physically narrow. GH-bearing sediments often contain primary detrital iron oxides: magnetite/titano-magnetite and hematite-ilmenite series minerals which remain unreacted in the presence of diagenetic greigite and pyrite. This assemblage is confirmed magnetically and petrographically (Esteban et al., 2010). The temporary (environmental) iron sulfide minerals

lie along a series of increasing sulfidation (Roberts and Turner, 1993) from mackinawite ($Fe^{2+}S^{2-}$) through greigite ($Fe^{2+}Fe_2^{3+}S_4$) and smythite (Fe_9S_{11}) to pyrite (FeS_2). Mackinawite is not observed in our 3 study areas, yet greigite/smythite and pyrite are common. Arguments concerning specific inorganic reaction pathways are only partially relevant because the predominant sulfide textures and habits appear to be mediated by bacteria. Whether we choose to describe the formation of the magnetic iron sulfides as a global statement like equation 3, or a stepwise process of precipitation and subsequent sulfidation reactions like equations 4 and 5, all of the reactants could originate from bacterial reduction of ferric iron and sulfate ions accompanying the anaerobic oxidation of methane (AOM) as per equation 1 above. Whether or not greigite arises via incomplete sulfidation on the path to pyrite as proposed by Sweeney and Kaplan (1973) (equations 4 and 5), pyrite is common in these GH settings and geologically seems to be the final product particularly where sulfide is abundant. In any case, the sulfur is supplied via ongoing bacterial sulfate reduction. Where sulfur is unlimited as near the seabed or with vigorous brine flux from below, greigite can be fully converted to pyrite via equation 6. There is textural evidence for this sulfidation process both as zonation of the iron sulfide minerals and the occurrence impure pyrite which is weakly magnetic where the conversion is incomplete.

MACKENZIE DELTA: PERMAFROST GH REGIME

Located along the coast of the Beaufort Sea, the Mackenzie delta sits in the Beaufort-Mackenzie foreland basin containing Cretaceous-Tertiary fluvial-deltaic sediments sourced from the Mackenzie mountains and Canadian shield. Two deep GH exploration wells were drilled, 100 m apart: the JAPEX/JNOC/GSC Mallik 2L-38 and 5L-38 (Dallimore and Collett, 2005; Fig. 2a). Cores were recovered from 886 and 953 m, and between 885 and 1152 m depth respectively, sampling three GH horizons, each about 35 m thick.

At the time of logging, the pore fluids were consistently fresh above the GH deposits and briney below, as seen in the well logs from Dallimore and Collett (2005). The overlying fresh waters seem to reflect the original pore waters, and the time average effects of meteoritic recharge and dilution from melted GH and permafrost. The underlying brine sets the lower stratigraphic limit for the GH deposits and is related to the salinity of advected basinal fluids in addition to higher salinity caused by solute expulsion during GH formation. Here, as in most sedimentary basins, density layering is normal. The whole formation housing the GH deposits is subjected to a flux of deep basinal fluids (fresh and briny) expelled along local fault conduits related to sediment compaction, tectonic loading and multi-ice-age deep permafrost conditions.

At Mallik, GH formation relates to climatic cooling during glacial intervals with downwards growth of the permafrost (Taylor, 1999 and Taylor et al., 2005), depressing the geothermal gradient to about 7°C/km (Dallimore and Collett, 2005). Freezing began from the surface, peripheral to continental ice sheets, during a succession of glacial maxima. The arctic climate setting has served not only to form three layers of permafrost GH, but also to preserve them for tens of thousands of years spanning warmer interglacial periods (Osadetz et al., 2005; Taylor et al., 2005). Local tectonic effects, the fluid flux and ice expansion give these unconsolidated sandy and silty sediments of the Mackenzie delta a dome-like structure (Fig. 3a) surrounded by faults, as previously studied by the petroleum industry and more recently for their GH energy potential (Osadetz et al., 2005). While the sediment deposition here has mainly been continental fluvial and deltaic, the sediment deposition for the overlying section above the GH deposits also includes coastal and marine deltaic facies at this location during interglacial sea level high-stands (Medioli et al., 2005).

At Mallik, the GH deposits are usually concentrated in unconsolidated channel sands or in veins and fractures which cut them where the porosity and permeability are the highest in the local sedimentary section. Here ordinary permafrost overlies GH (Fig. 3a) while free gas resides below. There is active methane venting to the surface from, through, and adjacent to this GH field. Elsewhere, in unfrozen locations, these characteristics are most similar to shallow gas fields in Tertiary continental fluvial sands. The GH is stable to depths of 1107 m. Carbonate and sulfide cemented siltstones and shales occur adjacent to continental fluvial sands and coals. Given the arctic setting and the lack of intervening unconformities, this is a highly unusual facies. The lower stratigraphic limit on the GH deposits (Fig.1, 3a) corresponds to the increasing geothermal gradient and underlying hyper-saline brines (Henninges et al., 2005).

The host sediments at Mallik are notably clean, composed of mature quartz arenites with fragments dominated by quartz-rich cherts and meta-quartzites (Fig. 5 a-e). The cements and leachate chemistry, from a series of weak organic acids up through nitric acid, are enriched in Ca, Mg, Fe, Mn, with unusual trace elements and rare earth elements (TES and REES) compared to the host sediments (Fig. 4). In weakly acidic solutions, labile ions are readily released to solution. This leachate composition is particularly significant in such a quartz-rich system because there is no detrital mineral source for most of the elements and the quartz just acts as a diluent. Pyrite, greigite (Fig. 5a, b) and dolomite (Fig. 5 c) oc-

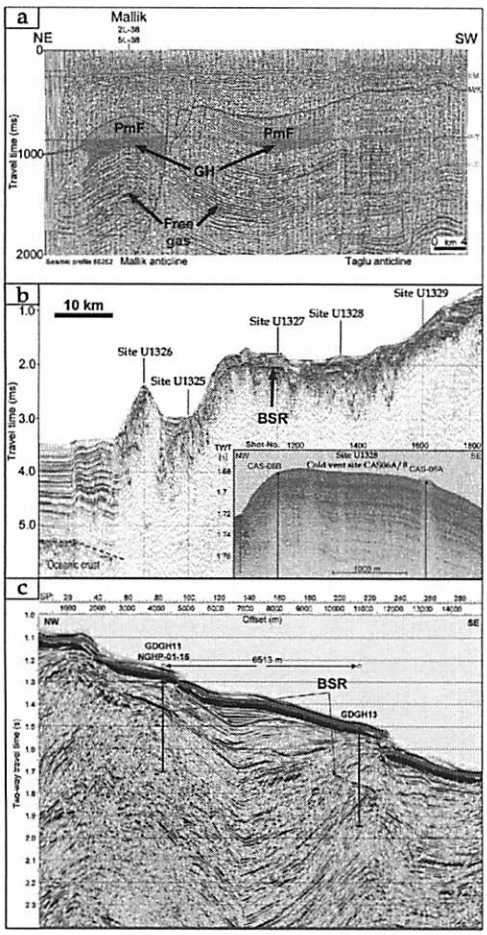

Figure 3: Seismic reflection profiles across three sites: (a) Mallik, (b) Cascadia Accretionary Wedge, and (c) Western Bengal (Krishna-Godavari) Basin. At Mallik (a) in the Pleistocene and older portion of the Mackenzie Delta ordinary ice permafrost (PmF) from about 600 m to 900 m sub-surface, corresponds to the lighter shading. The darker shading to about 1100 m sub-surface corresponds to gas hydrate (GH). The intense reflections deeper in the section are gas brightening due to free gas. The Cascadia accretionary margin (b) shows the bottom simulating reflector (BSR) at about 300 ms TWT into the seabed. Note how shallow the Pliocene basaltic ocean crust is in the lower left. The inset is a high resolution sub-bottom profile showing seismic blank zones (gas chimneys due to active methane venting) with cold vent sites 6a and b labeled on the inset. In the Krishna-Godavari basin (c) on the Indian passive margin, the multichannel seismic section shows the BSR within 0.15 s TWT of the seabed. Here, as on Cascadia, the gas hydrate occurs between the BSR and the seabed. The deeper dipping reflectors below about 1.8 s TWT depict the underlying Gondwana rifted margin sequence.

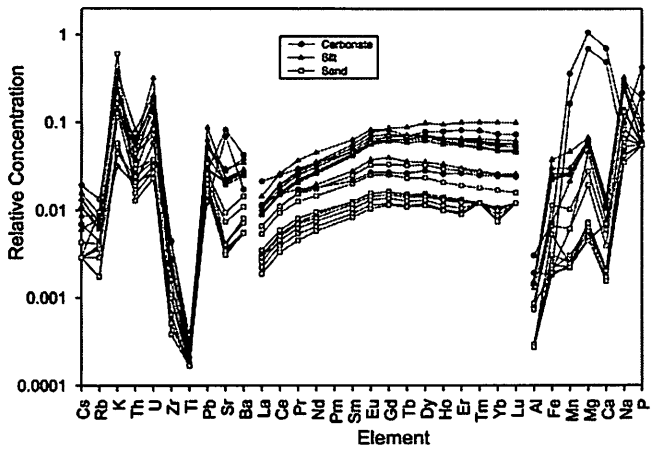

Figure 4: Geochemistry of the major and trace elements ICPMS (TES and REES) after the first 1 hour at pH 5.5 leach from representative samples at Mallik (carbonate, silt and sand lithologies). Data are normalized to GLOSS of Plank and Langmuir (1998). Quartz rich sands have lower concentrations of most elements compared to silts or carbonates due to the low cation exchange capacity and lower amount of labile ions. Notice the profound enrichment in Ca, Mg, Mn and Sr and the flatter rare earth patterns for the carbonate cemented samples reflecting the chemistry of transient pore waters.

cur as tensional vein fillings and as interstitial cements which split detrital grains and inflate primary sedimentary textures. The iron sulfide minerals overgrow detrital iron oxides and display no reaction texture. This suggests that there was another source for the iron in these cements rather than dissolving primary magnetite and hematite. Pyrite and the other iron sulfide minerals here are atypical in that they are enriched in Mn2+ to a total of several percent and they display a creamy bronze to pinkish-brown reflectance in polished sections (Fig. 5c-e).

The carbonate and sulfide cements are preferentially localized in the finer grained and least permeable silts (Fig. 5c), cementing them so thoroughly that they resemble hard, resistant, silty limestones in an otherwise unconsolidated section. Carbonates: (dolomite, siderite, ankerite and calcite), and sulfides (pyrite, smythite/greigite) nucleated and grew in pores, not at pore throats (Fig. 5c, f and g), and in cross cutting fractures. Successively introduced cements inflated original silts and crosscut earlier cement veins so extensively that they rafted detrital grains apart destroying original grain on grain contact, and fractured original detrital grains (Fig. 5 b, and d). The rock resembles limestone with a small proportion of isolated quartz silt grains. The adjacent GH bearing sands remain unconsolidated and show little or no mineral deposition, or sign of diagenetic cements. Where magnetic iron-sulfides (smythite/greigite) and pyrite are introduced, they enveloped or epitaxially overgrew detrital magnetites and ilmenites with no reaction (Fig. 5c, e and g).

The host sand and silt grains do not show the appropriate mineralogy, bulk composition or appreciable reaction textures to account for the diagenetically enriched elements in the carbonate and sulfide cements. These elements must have come along with advected lateral or vertical fluid flux via the same faults and permeability pathways which brought up the methane. In areas of concentrated local gas venting up through shallow modern distributary channels, such as the nearby NIG seep, there is sufficient CH_4 and SO_4^{2-} flux to completely reduce all primary detrital magnetite, creating local magnetic lows above the gas seeps (Esteban, et al., 2008).

Both the geological setting and the detailed characteristics of the cements at Mallik require tectonic fluid expulsion as a driving mechanism and control on the nature of the deposits and thus on the GH-related diagenesis. The change in fluid chemistry during cementation is clearly evident from carbonate cements which show both cathodo-luminescence and marked zonation in Mn content where dolomite succeeds earlier calcite as the principal carbonate cement mineral (Fig. 5 f, g). Pyrite has also overgrown earlier magnetic iron sulfides (FeS or Fe_3S_4) transforming the disseminated framboidal masses into mm to cm sized equant bladed grains with sieve-like internal tex-

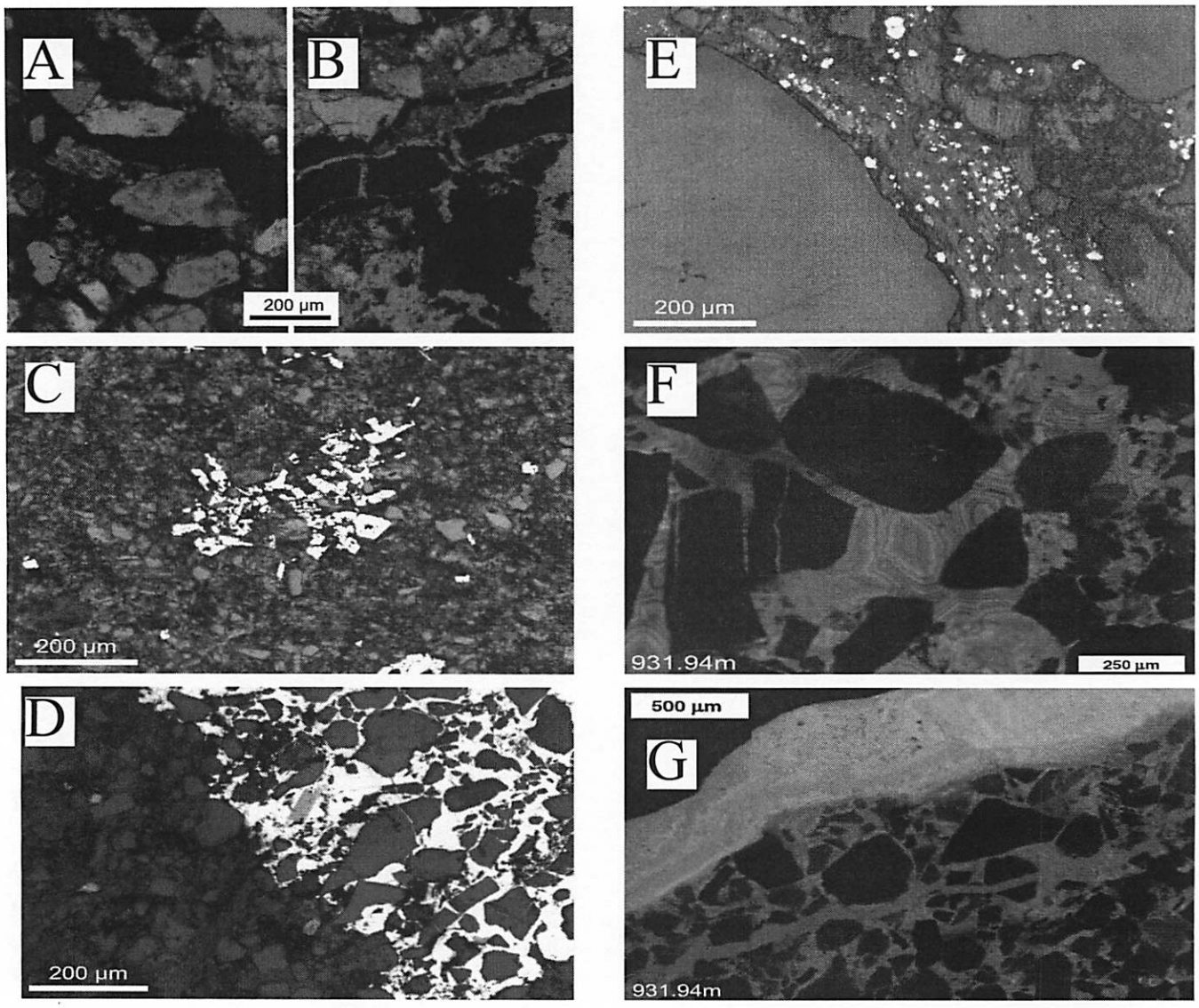

Figure 5: Thin section photomicrographs from Mallik. Figures (a) and (b) 108774 (1087.74 m depth): coarse quartz sand is cut by dark sulfide veins (Transmitted Polarized light). Fig. (b) Transparent carbonates rim and cross cut the sulfide veins. Fig. (c) 108740 (1087.4 m depth) is a silt shown in Reflected Plane Polarized Light (RPPL). Here, the highly reflectant greigite cement forms in cubes and bladed masses that overgrow the detrital clear angular quartz silt grains. Dark brown interstitial patches of zoned dolomite cement comprise more than 40% of this sample. Fig. (d) Sample 108662 (RPPL) has a bright creamy greigite overgrowth of detrital quartz and grey magnetite sand grains. Note the lack of reaction between greigite and euhedral magnetite and the vein and fracture infillings cutting detrital quartz. Fig. (e) 108774 (RTPL) in sand, shows multiple points of greigite nucleation along veins. Fig. 5 f, g 931.94 m from site 2L-38 cathodoluminescence photos from Medioli et al, 2005. The concentric zonation in (f) indicates nucleation in pore spaces, not pore throats, requiring saturation with respect to manganoan dolomite. The veins in (g) show multi-generation, zoned, and cross cutting Mn-bearing dolomite cements. Notice the fractured detrital quartz grains. This implies a tensile strength imparted to the unconsolidated sand by GH acting as a cement during vein emplacement.

ture and zonation towards the rims. The serial size range from small disseminations to large crystals also mimics textures of sedimentary massive sulfide deposits (SMS).

The multiple generations of carbonate and sulfide cements are texturally and chemically complex. They formed selectively, adjacent to the GH layers of porous sands and served to selectively lithify the adjacent less permeable silts. They also formed sequentially in a series of steps or pulses that caused fracturing as it delivered the fluids. The fracturing itself is enigmatic in this predominantly unconsolidated, and little cemented, succession. Nonetheless, fracturing is a common feature in many GH deposits, including those in offshore muds (Ruppel and Konoshita, 2000; Sassen et al., 2001; Flemings et al., 2003). Freezing of GH to impart some tensile strength and rapid pulses of fluid overpressures are both possible causes and possibly interdependent processes influencing diagenesis and mineral vein building in this setting. That five or more generations of cements occur in the space of a single thin section on the edge of a GH layer (Fig. 5a, b and g), suffice to demonstrate that this is a complex multi-generational deposit, and not the result of a single episode of fluid migration or the cooling effect from a single glacial interval.

CASCADIA ACCRETIONARY MARGIN: ACTIVE MARGIN UNDER GH REGIME

Located along the west coast of Vancouver Island in Canada (Fig. 2b), the Cascadia subduction margin forms an active accretionary wedge on a deep continental slope (Fig. 3b). It is capped by a neo-glacial dump of up to a few hundred meters thickness of fine-grained hemipelagic iceberg debris overlying Late Tertiary and Quaternary outer shelf and slope deposits. The outermost southwestern edge of this sediment wedge is deformed by folds and faults (Fig. 3b) related to convergence and offscraping of bathyal sediments over relatively warm, young and shallow seafloor of the Juan de Fuca-Explorer plate system (~6 Ma, age of seafloor at the outermost subduction zone thrust; Riddiough, 1984). The outer wedge is in tension, bowed upwards in a series of rotated folds and fault blocks with at least two different conjugate fault orientations that control the edges of massive slump blocks (Lopez, 2008). This deformation not only makes fluid migration pathways for expelled gas and brine but also actively creates structures and traps that can be charged to form GH deposits like the Bullseye vent (Riedel et al., 2002). Additionally, due to the very young age of the subducted seafloor here compared to 8 Ma or older further south along the Cascadia margin, there is also an increasing geothermal gradient both northwesterly along the subduction margin and seawards towards the SW from Vancouver Island (Hyndman and Wang, 1993).

The thin Tertiary shelf successions closer to the coast sit on a depressed geotherm and their kerogen is thermally immature, based on the Shell exploration wells drilled in the 1960's (Shouldice, 1971). By contrast, the outermost continental shelf and slope allows for the creation and emplacement of thermogenic gas into this part of the accretionary wedge. The neo-glacial dumps form a cap of relatively impermeable sediments deposited during the latest pulses of deglaciation, especially the Wisconsinan deglaciation of Vancouver Island and the Juan de Fuca Strait circa 14 ka ago (Clague and Brobowsky, 1999; Clague and James, 2002). Such sedimentological and geological conditions lead to:

-sudden loads applied to underlying sediments at the end of the Wisconsinan which cause compaction and fluid expulsion.

-an impermeable cap which allows gas to build up to high enough pore pressure for GH formation and which changes geo-mechanical properties of the wedge permitting tensile failures, slumps and faulting.

-a cap rock of deep cold carbonates which permits the build up free gas reservoirs just below

the GH and which may explain part of the impedance contrast responsible for the bottom simulating reflector (BSR).

Both the impermeable glacial deposits and more local build up of carbonate rock caps sufficiently retard the flux of methane to build up free gas reservoirs. This relatively young barrier collects enough methane gas to allow extensive bacterial growth, methane oxidation and growth of bacterially related carbonate and sulfide cements (Fig. 6a-g). These reactions occur from anoxic to suboxic environmental conditions beneath the seabed, and even under oxidizing conditions at the seabed. Once the GH and underlying free gas reservoirs form, ongoing deformations of the accretionary wedges create both tensile and shear features as ready conduits for methane flux to the seabed. Such methane/fluids vents are often detected by seismic blank zones with vertical offsets due to velocity push-down in the gassy core (Riedel et al., 2001; 2002). In some locations, active gas venting permeates the water column as seen on high frequency ocean sounding profiles (Fig. 3b; De Beukelaer et al., 2003; Vidalie, 2007). Active methane venting to the seabed along this portion of the deep outer continental shelf and slope (>1300 m) accesses the dissolved oxygen and unlimited sulfate of the deep ocean water, giving rise to bio-chemoherms with some resident benthic fauna pictured in Figure 7. Some of the carbonate mounds are more than 1.5 km across and 80m tall despite being in cold upwelling water undersaturated with respect to calcite and aragonite (Chen et al., 1988).

Methane vents on the Cascadia margin, manifest different styles of seabed geology depending on the flux, interaction with the water column and sedimentary substrates. Where methane vents directly to the ocean there is abundant dissolved oxygen for microbes to form carbonates and active bathyal biogeochemical mounds are formed (He et al., 2007). In Bullseye vent U1238 and CAS-06 (Fig. 2b, 3b) (Riedel et al., 2006) high methane flux leads to deposition of sulfides and reduced organics, as methane and sulfate exceed available iron from advected pore fluids and primary detrital minerals. There, GH deposits are observed directly at the seabed and deeper as massive layers inter-bedded with, and as veins cutting, glaciomarine sediments. Sediments within the vent area are blackened and carry higher organic carbon contents (Fig. 6a) than unaffected correlative sediments outside the vent (Novosel et al., 2005). In Barkley canyon, outcropping GH deposits have higher molecular weight hydrocarbons up to C-6 due to a deep predominantly thermogenic hydrocarbon source (Pohlman et al., 2005). This is essentially a frozen gas condensate reservoir. These hydrocarbons provide a viable food source for archaebacteria and have similar carbonate and sulfide cements, both mineralogically and isotopically, compared to GH deposits and seabed methane vents elsewhere as the biogenic mineral cements are the same.

The overview for Cascadia is that the carbonate and sulfide cements are predominantly calcite (Fig. 6d and e) and greigite plus pyrite (Fig. 6 b, c, d, e, and g). They are locally related to high primary porosity and sediment inflation from gas overpressures plus vertical tensional fractures, gash fractures and other open permeability pathways (Fig. 6b, c, d, e and f). The carbonate mounds and their sediment accumulations are most impressive with active methane venting through the seabed. Carbonates mounds occur usually as large build-ups on the Cascadia margin (He et al., 2007) but remain poorly studied in deep-water conditions (Henriet et al., 2001; Teichert et al., 2005). Complex communities from bacteria to invertebrates (gastropods, pelecypods, sea cucumbers) colonize (Fig. 7a and b) and construct mounds whose predominant texture is that of microbolite carbonate clasts; a classical bio-association in carbonate mud mounds (Van Dover et al., 2002; Campbell, 2006). Magnetic sulfide cements are present as lags near the seabed on the carbonate mounds where dissolution preferentially removes carbonate minerals, leaving a dark crust or ooze

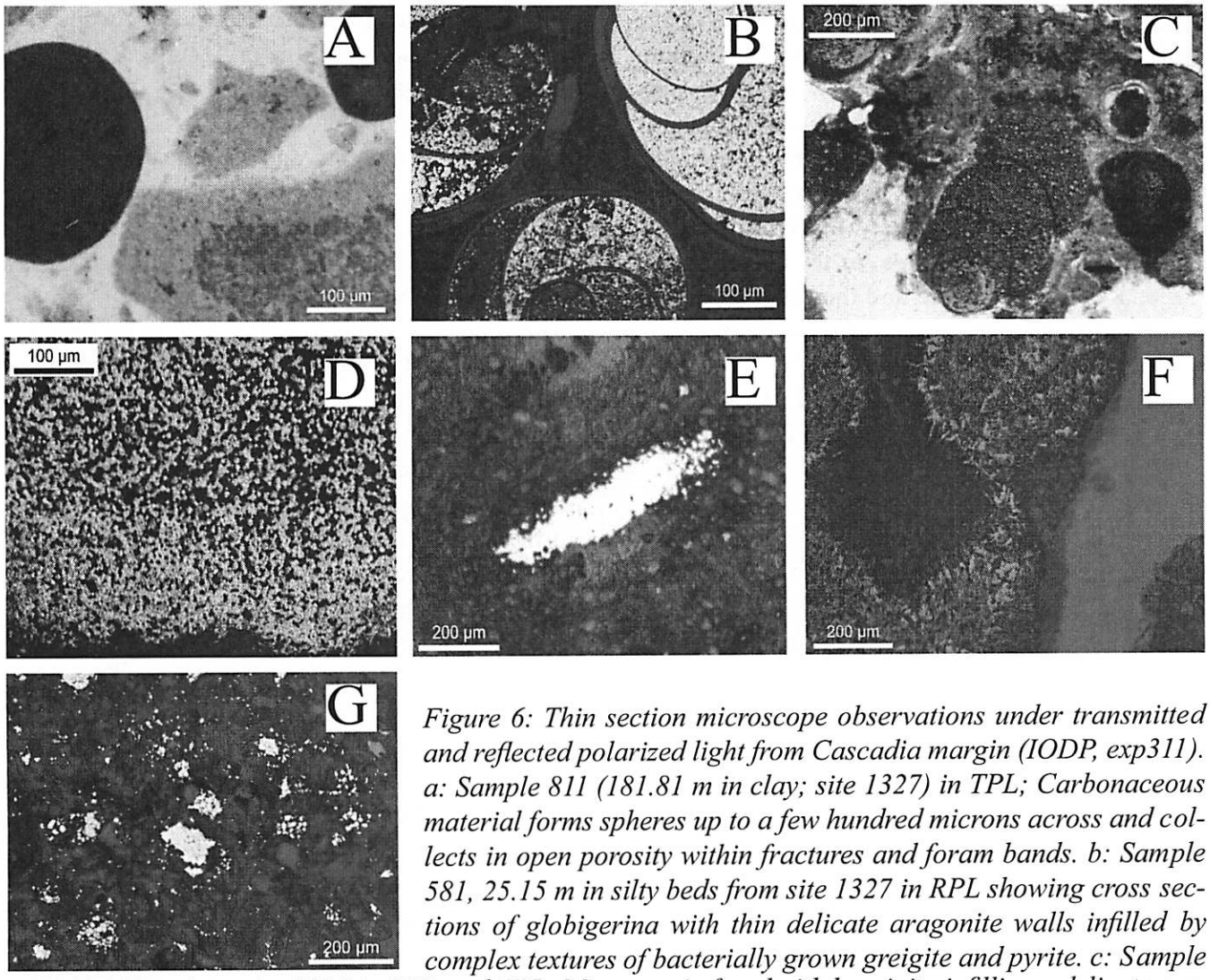

Figure 6: Thin section microscope observations under transmitted and reflected polarized light from Cascadia margin (IODP, exp311). a: Sample 811 (181.81 m in clay; site 1327) in TPL; Carbonaceous material forms spheres up to a few hundred microns across and collects in open porosity within fractures and foram bands. b: Sample 581, 25.15 m in silty beds from site 1327 in RPL showing cross sections of globigerina with thin delicate aragonite walls infilled by complex textures of bacterially grown greigite and pyrite. c: Sample 518, 237.95 m from site 1326 in RPL and TPL. Microscopic framboidal greigite infillings, delicate carbonate walled grobigerina tests, carbonaceous clots and glauconite are visible in the unconsolidated silty matrix. d: Sample 576, 22.65 m depth from site 1327 TPL image of a vein cross section. The unconsolidated silt at Cascadia is cut by lithified veins to several mm across which are infilled by swirled masses of very finely crystalline greigite (opaque) and carbonate material (birefringent). This composition suggests ample sulfate supply to produce sulfides and intricate bacterially controlled mineral deposition.e: Sample 319, 10.44 m from site 1326 in RPL and TPL of en echelon gash fractures of bright greigite cements are emplaced while original grey euhedral magnetite silt grains remain unaltered. f: Sample 811 (181.81 m in clay; site 1327) in RPL; Beneath the gas hydrate layer, needles and blades of smythite formed quickly around introduced carbonaceous matter and pierced the surrounding silt (glacial diamict). g. Sample 319, 10.44 m in silts with dropstones; site 1326 in RPL shows disseminated greigite and pyrite framboids which grew to larger than the original detrital silt grains. The rounded grey detrital magnetite grain to the right appears unreacted and is not the iron source for the sulfides.

near the seabed. The sulfides are more pervasive near GH deposits in the subsurface and seem texturally related to the migration of free gas especially where they occur in veins and fractures cutting unconsolidated sediment (Fig. 6d, e and f). Similar biogeochemical pathways and mineral end-products exist here as at Mallik but for Cascadia, the gas or fuel source for the bacteriogenic cements is both biogenic and thermogenic at different locations in the accretionary wedge.

KRISHNA-GODAVARI BASIN, BENGAL BASIN: PASSIVE MARGIN UNDER GH REGIME

The Krishna-Godavari Basin (KGB) represents the second most important terrigeneous fluvio-deltaic sediment supply to the Bengal basin (Indian Ocean; Biksham and Subramanian, 1988). It is located on a passive margin, along the east coast of continental India (Fig. 2c). This setting has been affected by rift and drift since the Cretaceous-Tertiary break-up of Gondwanaland (Curray et al., 1982; Alam et al., 2003). The deep sea Bengal fan is mainly composed of sediments coming from erosion of the Himalayas, uplifted during the Tertiary closure of the Tethys. The study area is located in deep waters on the continental slope within the distal delta fan, receiving sediments from two major rivers, the Krishna and the Godavari. Both carry sediment from the Cretaceous-Tertiary age basaltic Deccan traps of the Indian subcontinent; sediment which is particularly enriched in magnetite (Biksham and Subramanian, 1988).

The low elevation, low relief and dense vegetation related to the intense monsoon (Douglas et al., 1993), and the impermeablity of the Indian craton does not constitute a significant fluid head or pump into the offshore sediment wedge. This causes the KGB to be a very low flux system. The rifting phase of the passive margin was too long ago (K-T period) and is too deeply buried (Fig. 3c) to still be responsible for significant heat or fluid flux from the basement, despite the more recent loading of this crust by sediments of the KGB/Bengal fan (Abbas and Subramanian, 1984). The predominant fluid flux is confined to the post-rift sediments and is controlled by eustatic sea level changes and sediment pulses of the alternating glacial-interglacial climate cycle (Zachos et al., 2001; Clift, 2006). The pore fluids are thus limited to initial pore waters or minor flux from self-compaction in the KGB sediments. Due to detrital organics and woody plant matter in the sediments (Biksham and Subramanian, 1988), methane is formed within the sedimentary pile. The system is sulfide limited due to the initial pore fluid composition and lack of other inputs. Furthermore, the cements are spatially restricted and limited to textures typical of early diagenesis in the microporosity of woody plant fragments. This kind of early diagenetic cementation is common in other sedimentary settings, such as coal swamps, intertidal zones and soil profiles, where concretion formation or permineralization of biological detritus is related to solubility changes accompanying fluid flux or changing water tables, even in the absence of GH or methane flux. The high ratio of methane/sulfate due to high methane but low fluid flux (Collett et al., 2007), limits the methanotropic bacteria to incomplete oxidation and widespread deposition of fully blackend reduction carbon (Fig. 8a-c).

Polished sections have the reflectance of graphite and carbonized spherules are so pervasive as to impregnate whole intervals of the stratigraphy. Most magnetic iron sulfide growth is restricted to primary porosity in detrital coalified wood (Fig. 8 d) where partially oxidized organic molecules afforded faster or more complete bacterial oxidation. The carbonization of intervals in the KGB cores (Fig. 8a and c) is far more extensive than even the high methane flux regions on Cascadia like the Bullseye vent labeled U1328 and CAS-06b (Fig. 2b. 3b). The insight here is that the extensive carbonization and sulfide deposition are not signs of primary organic rich sedi-

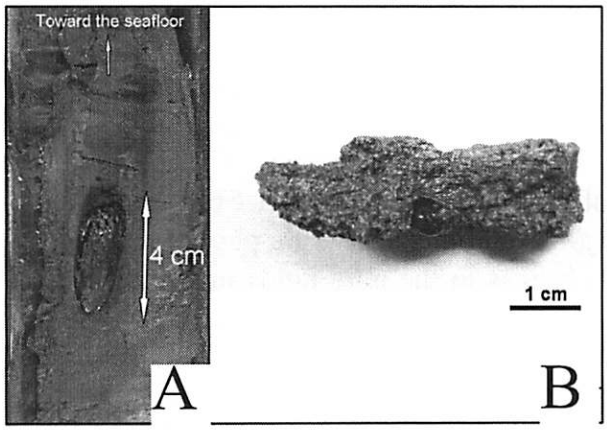

Figure 7: Living (leather clam) pelecypod in H2S bearing and sulfide and carbon stained glacial mud (a) and gastropod (b) in carbonate microbolite from a cold carbonate gas vent on the Cascadia Margin. The gastropod in (b) was grazing on bacterial colonies in this authigenic carbonate sand.

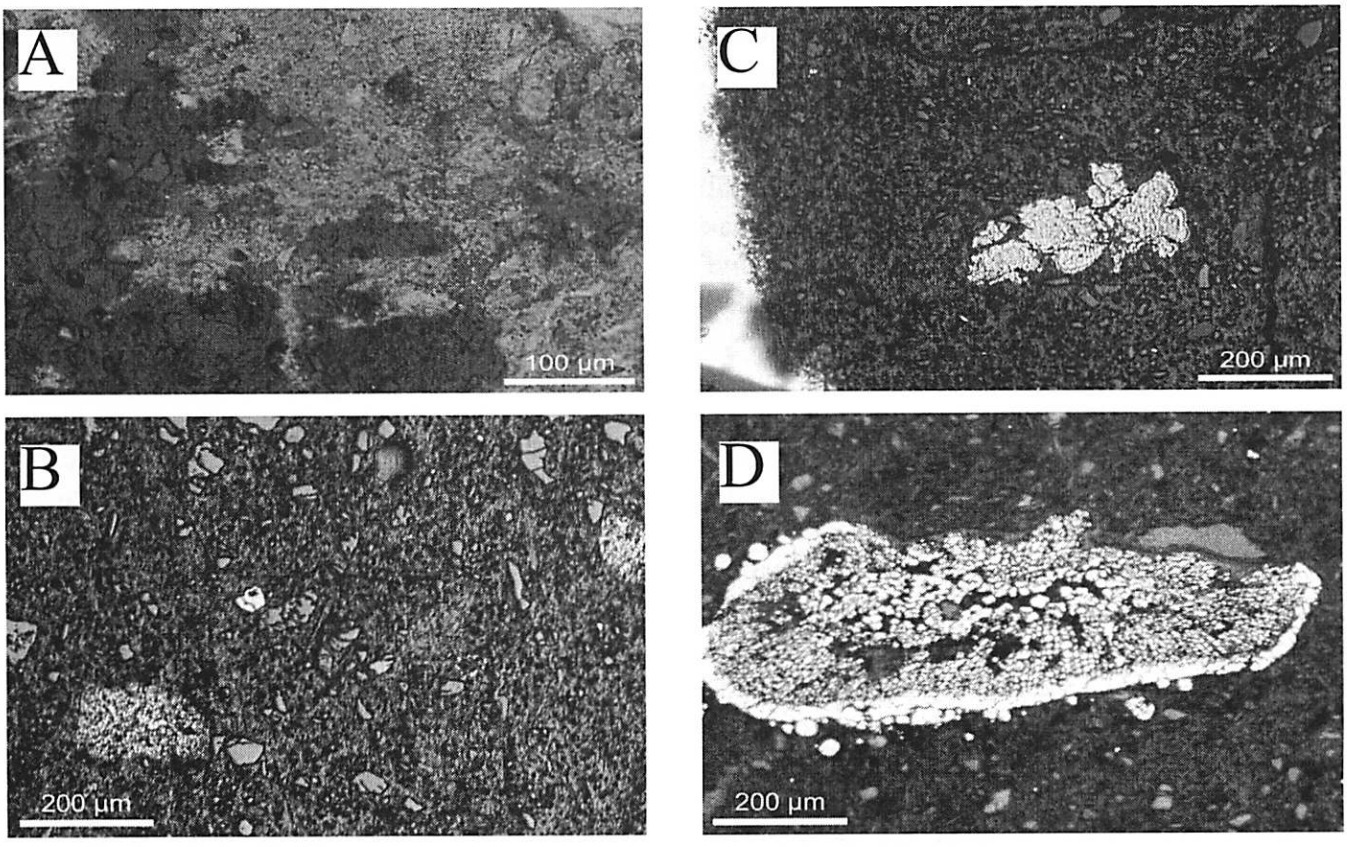

Figure 8: Thin section microscope observations under transmitted and reflected polarized light from the KGB (NGHP-exp01). (a) intense carbonization (black) of mud, with combined RPL and TPL light, (sample 333 at 80.7 m; site 7b&c); (b) and (c) sample 371 (160.3 m in silty sediments; NGHP sites 7b & c) are characterized an intensively carbonized matrix (> 90%) with 2 large greigite/pyrite clots with creamy reflectance and complex internal texture in (b) one massive colliform greigite clot in (c) with the occurrence of few large magnetites in grey; (d) sample 371 (160.3 m in silty sediments; NGHP site 5c) in RPL represents greigite replacing carbonized wood cells in a flattened stem.

ment, the productivity of the water column or an anoxic basin, instead, they result from vigorous methane flux and bacterial transformation of the KGB sediments after they were deposited.

DISCUSSION: METHANE FUELLED EARLY DIAGENESIS

Early diagenetic cementation fuelled by methanotrophic bacteria is irregular and incompletely developed in unconsolidated sediments from diverse GH settings. The controlling parameters are presented in Figure 9 as a sequential series of idealized stratigraphic columns through the sedimentary succession at Malik. In some locations, carbonate cements form, elsewhere iron sulfides form and at other sites yet, the sediments become carbonized. The sulfides are often magnetic iron-deficient mono-sulfides like greigite or smythite in disequilibrium assemblages with detrital magnetite. Sometimes, with progressive sulfidation, paramagnetic pyrite is all that remains and primary magnetite is gone. Examining the detailed mineralogy through three different GH occurrences provided a perspective on the critical pathways responsible for each disparate rock texture or mineral cement product. Those pathways are summarized in Figure 10. In most unconsolidated sediments, burial compaction and dewatering reduces porosity but causes little cementation or growth of new authigenic minerals. Some sediments contain organic detritus whether terrigenous or planktonic. These partially oxidized organic compounds (cellulose, organic acids, alcohols, esters, etc.) are readily oxidized under suboxic conditions at or near the sediment-water interface utilizing dissolved oxygen, sulfate or other oxy-anions. The limited diffusion of sulfate and its consumption by sulfate reducing bacteria can produce sulfide ions. These and the bicarbonate and carbonate ions from the oxidation of the organics provide half of the ions necessary to form carbonate and sulfide cements. Any oxy-anion complexes such as Mn^{3+}, $^{4+}$ (manganates) and Fe^{3+} (ferrates) are also reduced in sequence as alternative electron acceptors.

The low solubility of these species, particularly in brines, ensures the formation of greigite, calcite and dolomite cements. These provide the geologically persistent evidence of past fluid compositions and flux. There are physical and chemical changes to the pore fluids involving concentration, solution-dissolution and ion exchange processes, irrespective of inorganic or bacterially mediated redox reactions. Geochemists working with shallow sediment pore water profiles (Polhman et al., 2005) have demonstrated the common decrease in sulfate with depth in diverse seabed environments. This gradient is an ephemeral function of chemical diffusion and in situ consumption (conversion to sulfide) by sulfate-reducing bacteria. Sulfate and other oxidized ions can also be introduced by tectonic expulsion, compactional or thermal flux from the sediment column below or in short bursts by solute exclusion during gas hydrate crystallization (Jenner, et al., 1999).

In either shallow biofuelled redox reactions or deeper anoxic methane fuelled redox reactions, produced bicarbonate and sulfide ions are prevalent and available to form carbonate and sulfide mineral cements. While methane fuelled early diagenesis can operate in more diverse settings, here the cold, high pressure realm of gas hydrate introduces some important constraints and conditions. The formation of GH serves to cement unconsolidated sediments and makes a hydrocarbon reservoir that is also a secondary methane source, a permeability barrier and a cap-rock for free gas reservoirs below. Outside the GH stability field, methane flux may be insufficient to cause the proliferation of bacteria or their by-products. However, even at low methane flux, the GH permeability barrier can create a reservoir of free gas for methanotrophs to utilize creating their characteristic diagenetic mineral cements. Another physically unusual response is related to volume expansion on freezing. Ice or GH locally puts the section into tension at the same time as imparting a ten-

sile strength. Together, they allow the creation of open fluid and gas filled fractures in otherwise low strength unconsolidated sediments. Of particular note is the homogenization and cryoturbation of porous GH cemented sands. The profound fracturing and cement introduction adjacent to the GH reservoirs can expand original sediment to create micro-breccias and complex vein systems (Fig. 5).

The methane flux itself, whether shallow and biogenic as near the seabed in suboxic conditions, or deeper and thermogenic as in tectonic expulsion, affects the depth of the sulfate methane transition zone (SMTZ). If the methane flux occurs within the gas hydrate stability field (Fig. 1), GH can form with the aforementioned effects. In particular, even at low gas flux, once GH forms, methane can build up to create free gas (Fig. 3a). This built up methane creates a ready food source or substrate for archaebacteria. The incomplete development of the sulfide and carbonate mineral cements, their environmental magnetic overprints and existence of cold carbonate vent communities in cold deep sea settings undersaturated with respect to calcium carbonate has caused diverse interpretations as to the relative importance of processes and their effects. Although the development of this kind of early diagenesis is somewhat scattered and incomplete, still there is a sense to it once the controlling variables and their products are placed on a flow chart (Fig. 11). While Figure 10 is semi-stratigraphic in its presentation and development, there is no particular starting point or progression in Figure 11. Changing physical and chemical conditions place the strata and their mineralogy into a different box that might be anywhere on the chart (Fig. 11). This is especially true of real layered sedimentary sequences, long lived multi-ice age GH deposits and changing conditions (sea level, tectonics, faulting, freezing).

Methane must be available as a fuel or the sediments may compact but not cement in this way. Even if methane is available, where oxygen is limited below the sediment-water interface,

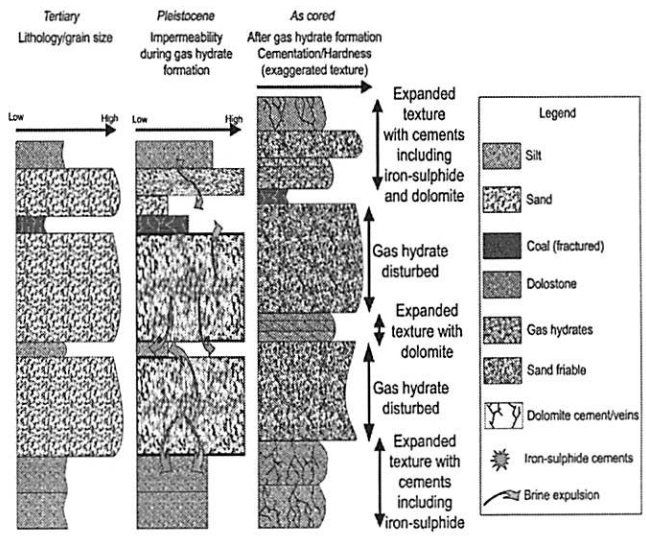

Figure 9: Model for gas hydrate crystallization and cementation in unconsolidated Tertiary sediments at Mallik. The left strip log shows the original character of the sediments with grain size increasing to the right. In the middle strip log, downwards cooling from permafrost and upwards methane flux forms GH in porous and permeable sands freezing them with appropriate volume increase into a GH cemented sandstone. As the GH takes only pure water, concentrated solutes are expelled along tensile fractures emanating from the GH deposit into adjacent less permeable beds. The right strip log shows the disturbed and partially cemented sediments as cored. Ice crystal formation in the GH layers often disturbs original cross bedding and other primary sedimentary structures sometimes destroying all sense of layering. Very hard beds of sulfide bearing silty dolostone are concentrated near the edges of GH horizons due to carbonate and sulfide ions that become concentrated there by expulsion or by the local products of anoxic methane metabolism.

bacterial oxidation can only occur in proportion to the availability of highly oxidized species such as sulfate or ferric iron. Without local electron acceptors the archaebacteria cannot proliferate. In places like the KG basin or the Bullseye vent in Cascadia, where methane flux is dominant and reductants are limited, high CH_4 / SO_4^{2-} ratios lead to incomplete oxidation of methane. The resulting production of carbon-rich reduced organic molecules persists after the bacteria, and paints the sediments black. On Cascadia, outside the vent areas, the glacio-marine sediments contain <0.5% total organic carbon (TOC) while in the blackened areas the same stratigraphy contains up to a few percent. This is a diagenetic pathway to create a reduced black shale or an organic rich source bed having a marine bacterial signature, without invoking an anoxic basin or a primary detrital organic load during that sediment cycle. Many seafloor massive sulfides (SMS) occur in black shales and in sections that are otherwise not anoxic. They may have developed by a process involving early methane fuelled diagenesis.

Where methane flux is low, or reductants are abundant, as near the seabed, carbonate mounds can form that are over 1 km across and many tens of meters high as in Cascadia. The textures of many of carbonate and sulfide cements

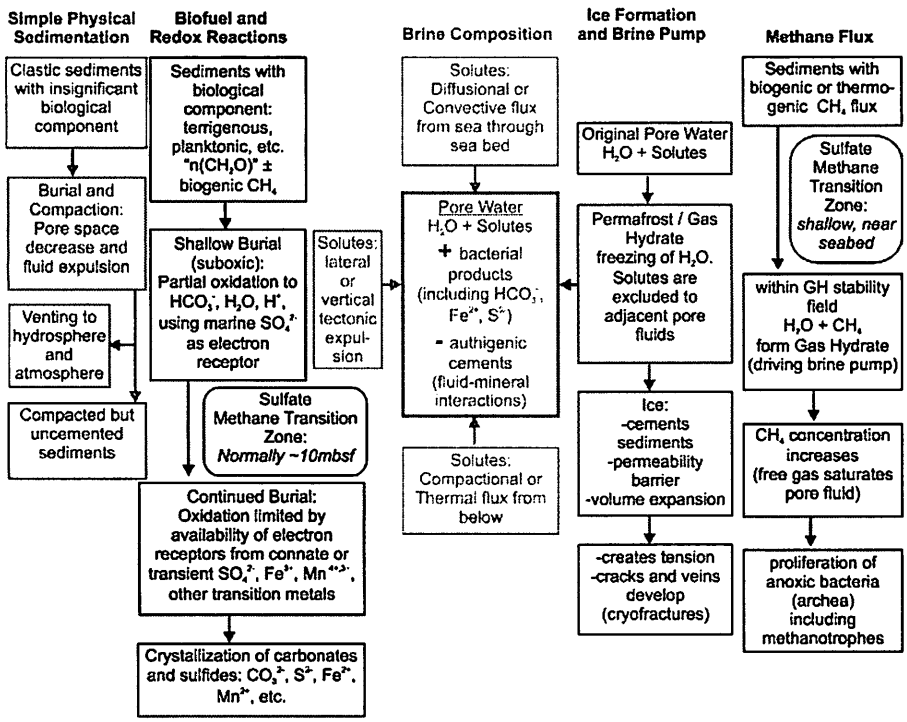

Figure 10: Elements of early methane fuelled diagenesis. The left column shows the ordinary burial compaction and fluid expulsion of unconsolidated sediments. The second column treats the influence of terrigeneous biofuel (cellulose, plankton, etc.) with suboxic conditions most detrital organic matter becomes reduced within a few meters below the seafloor. Deeper than this, the sulfate methane transition zone (SMTZ) controls the pore fluid chemistry and the precipitation of sulfide cements. The middle column deals with the fluid composition in the sediments. The pore water composition is controlled by several inputs including: initial pore fluid composition, descending diffusional or convective flow down through the seabed, solutes from below due to compaction or thermochemical advection via heat flow, solute flux from tectonic expulsion as in a foreland basin or active accretionary wedge and solute exclusion from nearby GH formation. The second column from the right outlines the physical role of ice formation in expelling brines and temporarily cementing and fracturing unconsolidated sediments, forming a permeability barrier. The final column on the right deals with the influence of methane flux. The three essential elements here are: that the flux affects the depth of the sulfate-methane transition zone (SMTZ); this in turn allows methane to build up and form GH, and finally the GH creates a permeability barrier or cap generating a free gas reservoir and permitting the growth of methanotrophic bacteria.

are microbial, even well into the subsurface and comprise further evidence that they are diagenetic rather than depositional.

Sulfate is the most important reductant in being able to form and preserve magnetic iron sulfide cements. If it is limited, as in the KG basin, the development of greigite cements is patchy and incomplete. This case describes the majority of the stratigraphic intervals at all three areas where the magnetic signals and petrography reveal a combination of the original detrital magnetic properties and incomplete diagenetic sulfide overprints. Bulk magnetic properties and microprobe analyses show that there is usually both some original detrital magnetite and some later diagenetic greigite present. Where fluid flux, mixing or diffusion provides unlimited sulfate, even the primary detrital magnetite is reduced to pyrite as at the Nig vent in the Mackenzie delta (Esteban et al., 2008). This is the natural and most common geological end-point with complete sulfidation of greigite to pyrite. In many of the shallow cores from Cascadia, this reaction is incomplete so pyrite is seen and predominant, yet it still contains sufficient early formed greigite to be readily separated by a hand magnet. While the original purpose of this study was to understand the formation of the magnetic iron sulfide cements, it seems intriguing that the methane fuelled sulfate reduction also explains a natural pathway to sulfidation for early diagenetic sediment hosted and deep marine SMS deposits.

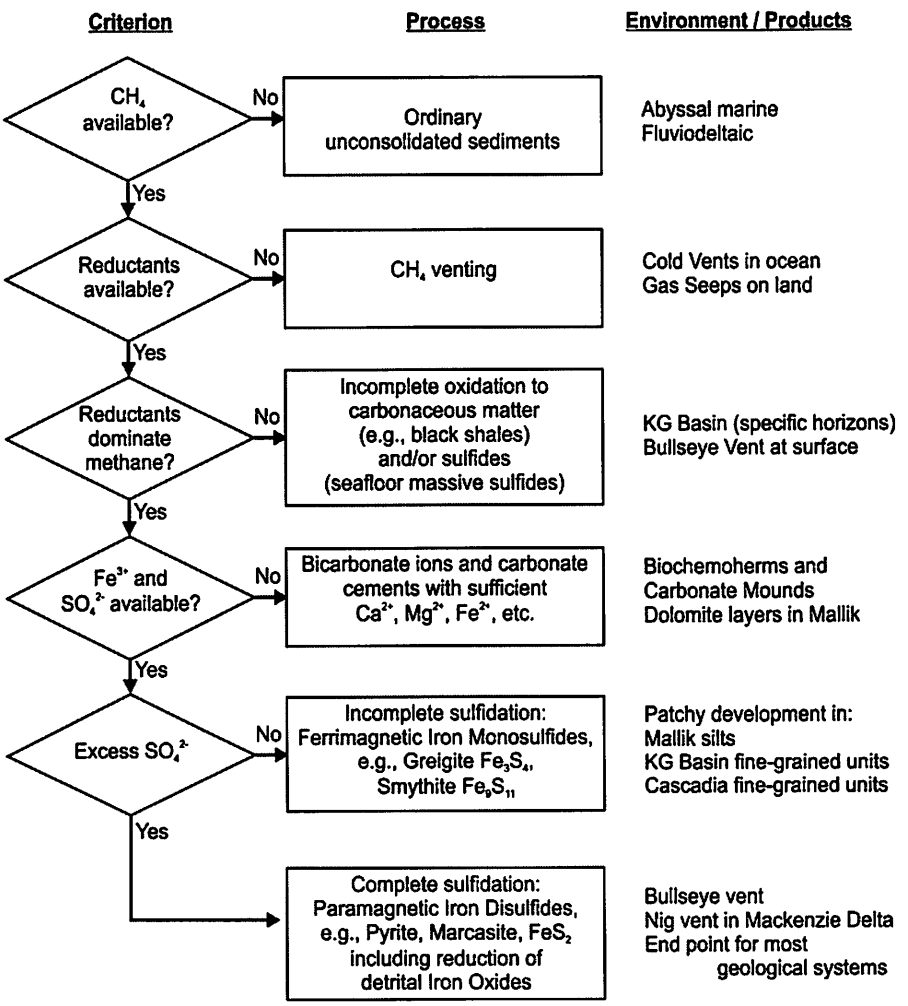

Figure 11: Flow chart depicting critical pathways for early methane fuelled diagenesis. From the diagenetic products observed at a site, the presence and balance between necessary chemical reactants can be inferred.

SUMMARY

The GH setting, whether beneath permafrost on a continental foreland basin, or marine on an active or a passive margin, affords a unique environment for a special type of methane-fueled, bacterially-related early diagenetic cementation. Here methane is a readily metabolized food source or fuel for primitive and ubiquitous archaebacteria present in the pore fluids of sediments. They produce mineral cements with complex bacterial textures, implying that simple inorganic expressions probably fail to capture the actual reaction mechanisms or fail to express the actual catalytic surfaces responsible for forming the magnetic iron sulfide cements. Since magnetite reduction is seldom observed in these settings, and greigite overgrows it without reaction textures, the source of the iron and sulfur is ultimately ions in aqueous solution. Where methane flux is moderate and the availability of oxidized components like sulfate or ferric iron is sufficient, complete oxidation of the carbon to carbonates and sulfidation of iron ions to magnetic iron sulfides and pyrite for the ultimate mineral products is commonly seen.

The edges of the GH deposits are particularly affected by these types of diagenetic cements and this is detectable both geophysically and petrologically. This is presumably due to the build up and availability of free gas at the GH margins due to its dissociation or the permeability barrier the GH represents and solute exclusion during freezing as we interpreted in Mallik (Fig. 9). Faults and pathways for methane and fluid venting are intensely affected by these processes where they provide the structural targets for high resolution aeromagnetic mapping and gas prospecting within the sedimentary section (Pierce et al., 1998). Where methane flux is pervasive, yet oxidized species are limited, incomplete oxidation of methane or bacterial products is responsible for carbonization of sediments. Perhaps the petrographic textures encountered in this study can serve as an atlas for methane-related early diagenetic cements elsewhere. While the cements are a small feature on the edges of the GH deposits, perhaps the local intensity of carbonate cementation even where calcite is undersaturated can testify to the importance of methane flux and bacterial processes in early sediment diagenesis and could explain some of the widespread reflectors interpreted as BSR by seismic methods. Similarly the high degree of sulfidation and carbonization in some of these horizons, and via this pathway involving methanotropic archaebacteria, can serve as a new model for the formation of some types of organic rich hydrocarbon source beds and some types of peridepositional sedimentary massive sulfide deposits.

ACKNOWLEDGEMENTS

This work is a combination and comparison of three different gas hydrate projects: Mallik, IODP 311, NGHP-01 and the 2009-007-PGC Tully cruise. We are deeply thankful to the entire cruise staff involved in the three offshore projects with special thanks to Michael Riedel, Scott Dallimore, Fred Wright and Tim Collett who were our scientific background advisers. Gwendy Hall and the GSC Geochemistry Lab are thanked for the help in the leachate geochemistry analysis as well as Matti Randsepp of the Electron microprobe Lab at the University of British Columbia, for the wavelength dispersive analyses of the sulfide cements. To finish, we are also grateful to Judith Baker and Ivana Novosel for help with the magnetic and physical properties measurements at the Geological Survey of Canada-Pacific Division Paleomagnetism and Petrophysics Lab.

REFERENCES

Abbas, N. and Subramanian, V., 1984. Erosion and sediment transport in the Ganges River basin, India: J. Hydrol., 69, 173-182.

Alam, M., Alam, M.M, Curray, J.R., Chowdhury, M.L.R. and Gani, M.R., 2003, An overview of the sedimentary geology of the Bengal Basin in relation to the regional tectonic framework and basin-fill history: Sedim. Geol., 155, 179-208.

Berner, R.A., 1970, Sedimentary pyrite formation: Am. J. Sci., 268, 1-23.

Biksham, G. and Subramanian, V., 1988, Sediment transport of the Godavari river basin and its controlling factors: J. Hydrol., 101, 275-290.

Blair, N.E. and Aller, R.C., 1995, Anaerobic methane oxidation on the Amazon shelf. Geochim. Cosmochim: Acta, 59, 3707-3715.

Campbell, K.A., 2006, Hydrocarbon seep and hydrothermal vent paleoenvironments and paleontology: Past developments and future research directions: Palaeogeogr. Paleoclimatol. Palaeoecol., 232, 362-407.

Clague, J.J. and James, T.S., 2002, History and isostatic effects of the last ice sheet in southern British Columbia: Quatern. Sci. Rev., 21, 71-87.

Clague, J.J. and Bobrowsky, P.J., 1999, The geological signature of great earthquakes off Canada's west coast: Geosci. Canada, 26, 1-15.

Chen, C.T.A., Feely, R.A., and Glendron, J.F. 1988. Lysocline, Calcium Carbonate Compensation Depth and Calcareous Sediments in the North Pacific Ocean. Pacific Science, 42: nos. 3-4, 237-252.

Clift, P.D., 2006, Controls on the erosion of Cenozoic Asia and the flux of clastic sediment to the ocean: Earth Planet. Sci. Lett., 241, 571-580.

Collett, T., Riedel, M., Cochran, J., Boswell, R., Presley, J., Kumar, P., Sathe, A., Sethi, A., Lall, M., Sibal, V., and the NGHP Expedition 01 Scientists, 2007: Indian National Gas Hydrate Program Expedition 01 initial reports. Directorate General of Hydrocarbons, New Delhi. CD ROM, Expedition 01 of the Indian National Gas Hydrate Program from Mumbai, India to Chennai, India: Sites NGHP-01-01 through NGHP-01-21, April 2006 – August 2006, Directorate General of Hydrocarbons, C-139, sector 63, Noida (V.P.) – 201301 India, www.dghindia.org, prepared by the United States Geological Survey.

Curray, J.R., Emmel, F.J., Moore, D.G. and Raitt, R.W., 1982, Structure, tectonics and geological history of the northeastern Indian Ocean. In: Nairn, A.E.M., Stehli, F.G. (Eds.), The Ocean Basins and Margins: The Indian Ocean, 6, Plenum, New York, 399-450.

Dallimore, S.R. and Collett, T.S., 2005, Summary and implications of the Mallik 2002 Gas Hydrate Production Research Well Program. In: Scientific Results from the Mallik 2002 Gas Hydrate Production Research Well Program, Mackenzie Delta, Northwest Territories, Canada, (ed) S.R. Dallimore and T.S. Collett: Geological Survey of Canada, Bull. 585.

De Beukelaer, S.M., MacDonald, I.R., Guinnasso, N.L. and Murray, J.A., 2003, Distinct sidescan sonar, RADARSAT SAR, and acoustic profiler signatures of gas and oil seeps on the Gulf of Mexico slope: Geo-Mar. Lett., 23, 177-186.

Dekkers, M.J. and Schoonen, M.A.A., 1996, Magnetic properties of hydrothermally synthesized greigite (Fe3S4). I. Rock Magnetic parameters at room temperature: Geophys. J. Int., 126, 360-368.

Douglas, W.B., Louis, A.D. and Christian, F.L., 1993, Reduced Himalayan sediment production 8 Myr ago despite an intensified monsoon: Nature, 364, 48-50.

Enkin, R.J., Baker, J., Nourgaliev, D., Iassonov, P. and Hamilton, T.S., 2007, Magnetic hysteresis parameters and Day plot analysis to characterize diagenetic alteration in gas hydrate-bearing sediments: J. Geophys. Res., 112, doi:10.1029/2006JB004638.

Esteban, L., Hamilton, T.S., Enkin, R.J., Lowe, C. and Novosel, I., in press, 2008, Gas hydrates and magnetism: Surveying and diagenetic analysis. In: Soc. Expl. Geophys., Special Vol., Seismic studies of Natural Gas Hydrate.

Flemings, P.B., Liu, X. and Winters, W.J., 2003, Critical pressure and multiphase flow in Black Ridge gas hydrates: Geology, 31, 1057-1060.

Fu, Y., Von Dobeneck, T., Franke, C., Heslop, D. and Kasten, S., 2008, Rock magnetic identification and geochemical process models of greigite formation in Quaternary marine sediments from the Gulf of Mexico (IODP Hole U1319A): Earth Planet. Sci. Lett., 275, 233-245.

Haq, B.U., 1998, Gas hydrates: greenhouse nightmare? Energy panacea or pipe dream? : GSA Today, 8, 2-6.

He, T., Spence, G.D., Riedel, M., Hyndman, R.D. and Chapman, M.R., 2007, Fluid flow and origin of a carbonate mound offshore Vancouver Island: Seismic and heat flow constraints: Mar. Geol., 239, 83-98.

Henninges, J., Schotter, J., Erbas, K. and Huenges, E., 2005, Temperature field of the Mallik gas hydrate occurrence – implications on phase changes and thermal properties. In: Scientific Results from the Mallik 2002 Gas Hydrate Production Research Well Program, Mackenzie Delta, Northwest Territories, Canada, (ed) S.R. Dallimore and T.S. Collett: Geological Survey of Canada, Bull. 585, 14 p.

Henriet, J.P., De Mol, B., Vanneste, M., Huvenne, V. and Van Rooij, D., 2001, Carbonate mounds and slope failures in the Porcupine basin : a development model involving fluid venting. In: Shannon, P.M., Haughton, P.D.W. and Corcoran, D. (Eds), The Petroleum Exploration of Ireland's offshore Basins: Geol. Soc. Special Publications, 188, 375-383.

Hensen, C., Zabel, M., Pfeifer, K., Schwenk, T., Kasten, S., Riedinger, N., Schultz, H.D. and Boetius, A., 2003), Control of sulphate porewater profiles by sedimentary events and the significance of anaerobic oxidation of methane for the burial of sulphur in marine sediments: Geochim. Cosmochim. Acta, 67, 2631-2647.

Hyndman, R.D. and Wang, K., 1993, Thermal constraints on the zone of major earthquake failure: the Cascadia subduction zone: J. Geophys. Res., 98, 2039-2060.

Jenner, K.A., Dallimore, S.R., Clark, I.D., Paré, D. and Medioli, B.E., 1999. Sedimentology of gas hydrate host strata from the JAPEX/

JNOC/GSC Mallik 2L-38 gas hydrate research well; in: Scientific Results from JAPEX/JNOC/GSC Mallik 2L-38 Gas Hydrate Research Well, Mackenzie Delta, Northwest Territories, Canada, (ed) S.R. Dallimore, T. Uchida and T.S. Collett: Geological Survey of Canada, Bull. 544, 57-68.

Krupp, R.E., 1994), Phase relations and phase transformations between the low-temperature iron sulfides mackinawite, greigite, and smythite: Eur. J. Mineral., 6, 265-278.

Kvenvolden, K.A., 1993, Gas hydrates-geological perspective and global change: Rev. Geophys., 31, 173-187.

Lee, S.Y. and Holder, G.D., 2001, Methane hydrates potential as a future energy source: Fuel Process. Techno., 71, 181-186.

Lopez, C., 2008, Seismic structure associated with gas hydrate at the frontal ridge of Northern Cascadia margin: MSc, Univ. Victoria, Victoria, BC, Canada.

Medioli, B.E., Wilson, N., Dallimore, S.R., Paré, D., Brennan-Alpert, P. and Oda, H., 2005, Sedimentology of the cored interval, JAPEX/JNOC/GSC et al. Mallik 5L-38 gas hydrate production research well. Scientific Results from the Mallik 2002 Gas Hydrate Production Research Well Program, Mackenzie Delta, Northwest Territories, Canada, (ed) S.R. Dallimore and T.S. Collett: Geological Survey of Canada, Bull. 585.

Novosel, I., Spence, G.D. and Hyndman, R.D., 2005, Reduced magnetization produced by increased methane flux at a gas hydrate vent: Mar, Geol., 216, 265-274.

Osadetz, K.G., Morrell, G.R., Dietrich, J.R., Snowdon, L.R., Dallimore, S.R. and Majorowicz, J.A., 2005, Beaufort-Mackenzie Basin: a review of conventional and nonconventional (gas hydrate) petroleum reserves and undiscovery resources. In: Scientific Results from the Mallik 2002 Gas Hydrate Production Research Well Program, Mackenzie Delta, Northwest Territories, Canada, (ed) S.R. Dallimore and T.S. Collett: Geological Survey of Canada, Bull. 585.

Paull, C.K., Ussler, W.III. and Dillon, W.P., 1991, Is the extent of glaciation limited by marine gas-hydrates: Geophys. Res. Lett., 18, 432-434.

Peirce, J. W., Goussev, S. A., Charters, R. A., Abercrombie, H. J., and DePaoli, G. R., 1998, Intra-sedimentarymagnetization by vertical fluid flow and exotic geochemistry: The Leading Edge, 17, 89-92

Plank, T., and Langmuir, C.H. (1998), The chemical composition of subducting sediment and its consequences for the crust and mantle, Chem. Geol., 145, 325–394.

Pohlman, J.W., Canuel, E.A., Chapman, N.R., Spence, G.D., Whiticar, M.J. and Coffin, R.B., 2005, The origin of thermogenic gas hydrates on the northern Cascadia Margin as inferred from isotopic (13C/12C and D/H) and molecular composition of hydrate and vent gas: Organic Geochem., 36, 703-716.

Pyzik, A.J. and Sommer, S.E., 1981, Sedimentary iron monosulfides: kinetics and mechanism of formation: Geochim. Cosmochim. Acta, 45, 687-698.

Riddiough, R.P., 1984, Recent movements of the Juan de Fuca plate system: J. Geophys. Res., 89, 6980-6994.

Riedel, M., Spence, G.D., Hyndman, R.D. and Chapman, N.R., 2002, Seismic investigations of an apparent active vent field associated with gas hydrates offshore Vancouver island: J. Geophys. Res., 107, 1-16.

Riedel, M., Spence, G.D., Chapman, R.N. and Hyndman, R.D., 2001, Deep sea gas hydrates on the Northern Cascadia margin: Lead. Edge, 20, 87-91.

Riedel, M., Novosel, I., Spence, G.D., Hyndman, R.D., Chapman, R.N., Solem, R.C. and Lewis, T., 2006, Geophysical and geochemical signatures associated with gas hydrate–related venting in the northern Cascadia margin: Geol. Soc. Am. Bull., 118, 23-38.

Riedinger, N., Pfeifer, K., Kasten, S., Garming, J.F.L., Vogt, C. and Hensen, C., 2005, Diagenetic Alteration of Magnetic Signals by Anaerobic Oxidation of Methane Related to a Change in Sedimentation Rate: Geochim. Cosmochim. Acta, 69, 4117-4126.

Roberts, A.P., 1995, Magnetic properties of sedimentary greigite (Fe3S4): Earth Planet. Sci. Lett., 134, 227-236.

Roberts, A.P. and Turner, G.M., 1993, Diagenetic formation of ferrimagnetic iron sulphide minerals in rapidly deposited marine sediments: South island, New Zealand: Earth Planet. Sci. Lett., 115, 257-273.

Ruppel, C. and Kinoshita, M., 2000, Fluid, methane, and energy flux in an active margin gas hydrate province, offshore Costa Rica: Earth Planet, Sci. Lett., 179, 153-165.

Sassen, R., Losh, S.L., Cathles, III, L., Roberts, H.H., Whelan, J.K., Milkoc, A.V., Sweet, S.T. and DeFreitas, D.A., 2001, Massive vein-filling gas hydrate: relation to ongoing gas migration from the deep subsurface in the Gulf of Mexico: Mar. Petrol. Geol., 18, 551-560.

Shouldice, D.H., 1971, Geology of the western Canadian continental shelf: Can. Soc. Petrol. Geol. Bull., 19, 405-424.

Sloan, E. D., Jr., 1998, Clathrate hydrates of natural gases: Second edition, Marcel Dekker Inc.: New York.

Sweeney, R.E. and Kaplan, I.R., 1973, Pyrite framboid formation: laboratory synthesis and marine sediments: Econ. Geol., 68, 618-634.

Taylor, A.E., 1999, Modelling the thermal regime of permafrost and gas hydrate deposits to determine the impact of climate warming, Mallik field area. In: Scientific Results from JAPEX/JNOC/GSC Mallik 2L-38 Gas Hydrate Research Well, Mackenzie delta, Northwest Territories, Canada, (Ed.) S.R. Dallimore, T. Uchida, and T.S. Collett: Geological Survey of Canada, Bull. 544, 391-401.

Taylor, A.E., Dallimore, S.R., Hyndman, R.D. and Wright, F., 2005, Comparing the sensitivity of permafrost and marine gas hydrate to climate warming. In: Scientific Results from the Mallik 2002 Gas Hydrate Production Research Well Program, Mackenzie Delta, Northwest Territories, Canada, (ed) S.R. Dallimore and T.S. Collett: Geological Survey of Canada, Bull. 585, 11 p.

Teichert, B.M.A., Bohrmann, G. and Suess, E., 2005, Chemoherms on Hydrate Ridge – Unique microbially-mediated carbonate build-ups growing into the water column: Paleogeogr. Paleoclimatol. Paleoecol., 227, 67-85.

Van Dover, C.L., German, C.R., Speer, K.G., Parson, L.M. and Vrijenhoek, R.C., 2002, Evolution and biogeography of deep-sea venting and seep invertebrates: Science, 295, 1253-1257.

Vidalie, M., 2007, Methane bubble plumes on the northern Cascadia margin detected by echo sounder: Internship report, Natural Resources Canada, Pacific Geoscience Center, Sidney, BC, Canada and Ecole Normale Supérieure, Magistère, TAO, Paris France. 42p.

Zachos, J., Pagani, M., Sloan, L., Thomas, E. and Billups, K., 2001, Trends, rhythms and aberrations in global climate 65 Ma to Present: Science, 292, 686-693.